DISASTER PREVENTION FUNCTION OF NOURISHED BEACH DURING 50 YEARS UNDER CONDITIONS OF SEA LEVEL RISE AND LAND SUBSIDENCE

Yoshiaki Kuriyama[1, 2], Hiroyuki Hayashi[3], Souichi Yamagata[4], Toshihiro Shimizu[5], Akiyoshi Katano[6], Haruo Mori[1] and Shusei Ogawa[7]

The disaster prevension function is oen of the key functions that sandy beaches offer. This study investiagted whether a nourided beach at the Niigata West Coast in Japan, which previously suffered severe beach erosion, can maintain its disaster prevention function for a 50-year period under conditions of sea level rise and land subsidence. At the study beach, which is now surrounded by submerged breakwaters and groins, beach nourishment was implemented from 1994 to 2000. This study defined the disaster prevention function as the ability to prevent the wave runup height induced by the design wave from exceeding the level of the road located immediately landward of the beach at the high high water level. The critical beach width, which is the minimum width required to satisfy the criterion for the disaster prevention function, was determined by estimating wave runup heights on several assumed eroded breach profiles and by evaluating the estimated wave runup heights exceed the road level. Future shoreline change was predicted using a numerical model under a sea level rise of 4.1 mm/year, which is the value for the RCP2.6 scenario, and a land subsidence of 7.0 mm/year. The comparison between the prediction results and the critical beach width confirmed that the disaster prevention function at the study beach is expected to remain effective for the next 50 years starting from 2019 even under conditions of sea level rise and land subsidence.

Keywords: sandy beach; backshore; wave runup; beach nourishment; climate change; RCP2.6

INTRODUCTION

Sandy beaches serve various functions, one of which is disaster prevention. Beaches dissipate wave energy through wave breaking, reducing wave runup heights and wave overtopping rates, thereby protecting residents, properties and infrastructure behind the beaches. When an artificially nourished beach is constructed as a countermeasure against beach erosion, a key concern is the durability of its disaster prevention function, particularly in the context of sea level rise due to global warming.

The objective of this paper is to investigate whether a nourished beach at the Niigata West Coast in Japan, which previously suffered severe beach erosion (e.g., Kuriyama et al., 2006), can maintain its disaster prevention function for a 50-year period under conditions of sea level rise and land subsidence.

In this study, first, the disaster prevention function is defined. Second, the critical beach width of the beach, which is the minimum width required to satisfy the criterion for the disaster prevention function, is determined. Third, the future shoreline change of the beach for the next 50 years is predicted using a simulation model and compared with the critical beach width.

STUDY SITE

The Niigata West Coast is located in central Japan and faces the Sea of Japan (Figure 1). The coast was formed by sediments discharged from the Shinano River, the longest river in Japan. However, owing to a decrease in sediment discharge due to openings of two diversion channels and the interruption of longshore sediment transport due to the construction of a jetty and a breakwater, the coast suffered severe beach erosion since the 1910s (e.g., Kuriyama et al. 2006).

As countermeasures against the erosion, a number of detached breakwaters were constructed since the 1950s and they safely protected beaches behind them. However, seaward of the breakwaters, the erosion continued and was considered a threat to the stability of the breakwaters. Thus, to prevent this erosion, submerged breakwaters have been installed at a distance of approximately 350 m from the shore since 1989 along with groins that have been in place since 1988. Beach nourishment started in 1994 and all of the construction work was completed in 2023.

The Niigata West Coast was divided into 5 sections (Figure 1) and Section A was selected as the investigation area. In Sections A, B, C and D, the submerged breakwater has an alongshore length of

[1] Coastal Development Institute of Technology, Japan. kuriyama_y@cdit.or.jp
[2] Port and Airport Research Institute, Japan.
[3] Civil Aviation Bureau, Ministry of Land, Infrastructure, Transport and Tourism, Japan.
[4] The Ports and Harbours Association of Japan, Japan.
[5] Hokuriku Regional Development Bureau, Ministry of Land, Infrastructure, Transport and Tourism, Japan.
[6] Ecoh Co., Ltd., Japan.
[7] HONMA Corporation, Japan.

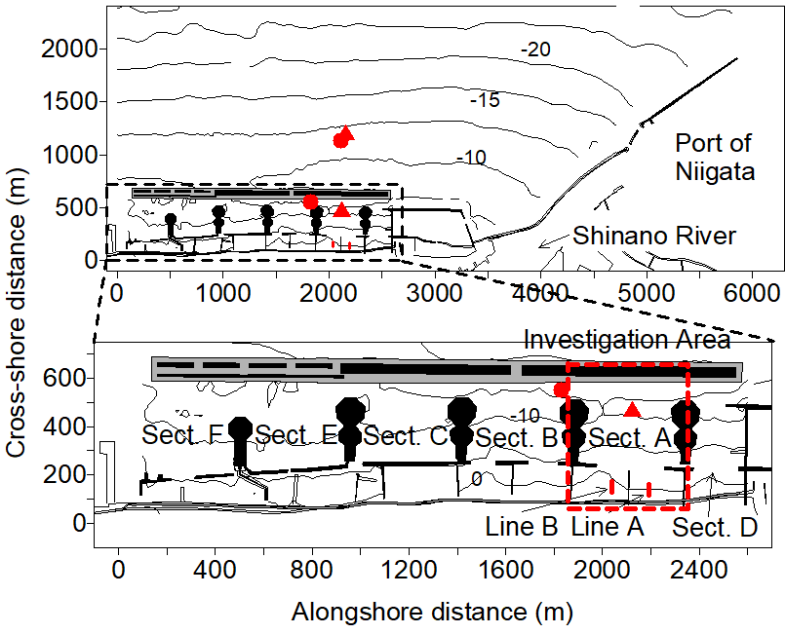

Figure 1 Investigation area and locations of wave gauges installed in 2012 (red triangles) and 2014 (red circles). Lines A and B (red lines) are the survey lines in 2014. Line A is also used in the 2021 video measurement.

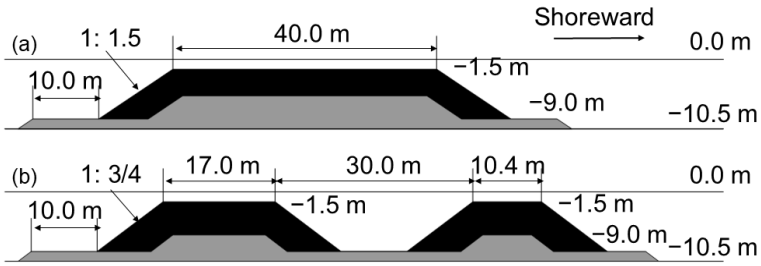

Figure 2 Structures of submerged breakwaters with (a) single crown and (b) double crowns.

1,630 m and a cross-shore width of 40.0 m (Figure 2). The crown height was designed at 1.5 m below the water level, but it is currently approximately 2.5 m below the low water level. In Section B, the submerged breakwater features a 50-meter opening. Sections E and F contain another submerged breakwater, which has two crowns with cross-shore widths of 17.0 m and 10.4 m (Figure 2) and an alongshore length of 760 m (Kishi et al., 2013). This design was intended to enhance alongshore flow in the gap between the crowns, reducing the amount of wave setup over the submerged breakwater, which can induce severe erosion immediately shoreward of a submerged breakwater as shown in Kuriyama et al. (2006). The nourishment was implemented in three sections: in Section A from 1994 to 2000, Section B from 2001 to 2008 and Section D from 1998 to 2008.

Offshore waves were measured at a water depth of approximately 35 m (139°07′34″E, 38°00′17″N). The monthly mean offshore significant wave height during a period from 2001 to 2019 exceeded 1.5 m from December to February, but it was below 0.5 m from June to August (Figure 3). The monthly mean offshore significant wave period ranged from 4.6 s to 7.1 s. The offshore significant wave height and period for waves with an occurrence probability of five times per year were 4.5 m and 9.5 s, respectively. Those of the design wave, which has an occurrence probability of once every 50 years, were 9.30 m and 14.3 s, respectively. The tidal data were offered by Japan Oceanographic Data Center. The low, high and high high water levels are 0.0 m, 0.50 m and 0.88 m, respectively. The median sediment diameter ranged from 0.14 to 0.30 mm. The morphology at the study site was basically surveyed biannually. The elevation z was defined relative to the low water level, which shifts according to sea level rise due to global warming.

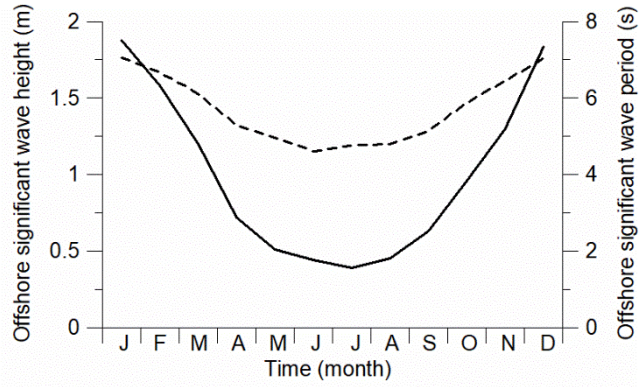

Figure 3 Monthly mean offshore significant wave height (solid line) and period (broken line).

DEFINITION OF DISASTER PREVENTION FUNCTION

The disaster prevention function was defined as the ability to prevent the wave runup height induced by the design wave from exceeding the level of the road located immediately landward of the beach at the high high water level. The road level in Section A was 4.0 m.

METHODS

Determination of critical beach width

The critical beach width was determined by estimating wave runup heights at the shoreward edges of the backshores of assumed eroded beach profiles (mentioned below) using the modified hypothetical slope method for composite type beach profiles developed by Nakamura et al. (1972) and by evaluating whether the estimated wave runup heights exceed the road level. The modified hypothetical slope method is based on the results of model experiments using regular waves. Thus, this method was calibrated using field data (mentioned below). In the estimation of the wave runup height, the wave height reduction and wave setup due to wave breaking over the submerged breakwater were calculated by Eqs. (1) and (3), respectively.

Nearshore wave transformation from offshore to the seaward edge of the submerged breakwater

First, without considering wave breaking, nearshore wave transformation from offshore to the seaward edge of the submerged breakwater was calculated using a numerical model based on energy balance equation. Then, using the equivalent deepwater wave height at the seaward edge of the submerged breakwater and the Goda's formula for wave height estimation in the surf zone (Goda, 1985), the wave height at the seaward edge of the submerged breakwater was estimated.

Wave height reduction and wave setup over the submerged breakwater

The wave height reduction and the mount of wave setup $\overline{\eta}$ due to wave breaking over the submerged breakwater were estimated using Eqs. (1) and (3), respectively, which were proposed by Takayama et al. (1988) based on model experiments.

$$H_2 = K_H H_1 \frac{K_{s2}}{K_{s1}} \qquad (1)$$

$$K_H = -0.92\frac{B}{L_0} + 0.42\frac{h_{SB}}{H_0'} + 3.8\frac{H_0'}{L_0} + 0.51 \quad (2)$$

where H is the significant wave height, K_s is the shoaling coefficient, B is the width of the submerged breakwater, L_0 is the offshore wavelength corresponding to the significant wave period, h_{SB} is the water depth over the submerged breakwater without consideration of wave setup, H_0' is the equivalent deepwater significant wave height. The subscripts 1 and 2 denote the values seaward and shoreward of the submerged breakwater, respectively.

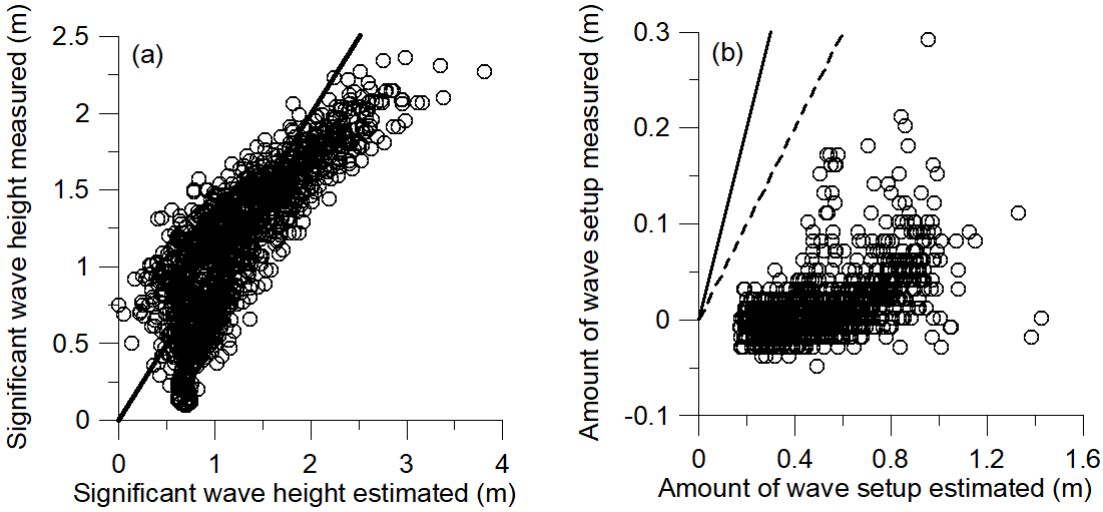

Figure 4 Comparisons between the measured and estimated values shoreward of the submerged breakwater for (a) the significant wave height and (b) the amount of wave setup. The solid lines represent perfect agreements and the broken line in panel (b) represents the relationship where the measured values are half of the estimated values.

$$\overline{\eta} = K_e H_0' \quad (3)$$

$$K_e = 0.085\frac{B}{L_0} + 0.16\frac{h_{SB}}{H_0'} + 0.38\frac{H_0'}{L_0} + 0.125 \quad 0 < h_{SB}/H_0' \leq 0.5$$

$$K_e = 0.048\frac{B}{L_0} + 0.056\frac{h_{SB}}{H_0'} - 0.21\frac{H_0'}{L_0} + 0.076 \quad 0.5 < h_{SB}/H_0' \quad (4)$$

To confirm the validity of the formulae, field measurements on wave transformation and wave setup over the submerged breakwater were conducted at a frequency of 2 Hz for 20 minutes at 1-hour intervals from November 2012 to January 2013 using wave gauges installed seaward and shoreward of the submerged breakwater (see the locations in Figure 1).

The comparison between the significant wave heights shoreward of the submerged breakwater measured and estimated from Eq. (1) shows that the estimated values nearly agree with the measured values (Figure 4 (a)); the root-mean-square error was 0.34 m.

The amount of wave setup estimated from Eq. (3) were larger than the measured values (Figure 4 (b)). A design manual of artificial reefs published in Japan (Seacoast Office of River Bureau of Ministry of Land, Infrastructure, Transport and Tourism, and Coast Division of National Institute of Land and Infrastructure Management, 2004) reported that the amount of wave setup over a submerged breakwater in the field is mostly less than half of the value estimated based on 2DV model experiments. In the measurement at the study site in 2012 to 2013, the measured values did not exceed half of the values estimated from Eq. (3). Thus, we used the upper limit, half of the value estimated from Eq. (3), as the estimated amount of wave setup.

Calibration of modified hypothetical slope method

The modified hypothetical slope method was calibrated using two sets of field data: video images of wave runup on the foreshore taken in March 2021 and topographic data on a beach scarp on the foreshore caused by a severe storm in December 2014 (Okuda et al., 2017).

In the video measurements, six poles were installed at about 3 m intervals between z = 1.33 m to 3.85 m along Line A (see the location in Figure 1). Six 20-minute measurements were conducted on March 2 and 3, 2021. Video images as shown in Figure 5 were captured at a rate of one per second. The offshore significant wave heights and periods along with the tides during the measurements are listed in Table 1. In the estimation of wave runup heights, the beach profile measured in June 2020 was used.

The wave runup height in the field under irregular wave conditions was given by $R_{2\%}$ as in EurOtop (2018), which is the value exceeded by 2 % of the number of incident waves. Since the number of waves during the 20-minute measurements estimated from the significant wave period ranging from 8.5 s to 9.7 s was 124 to 141, $R_{2\%}$ was defined as the third largest wave runup height.

Figure 5 Photo of wave runup on the foreshore taken on 2 March, 2021.

Table 1 Offshore significant wave heights and periods and tides during the measurements in 2021.

Start time	Wave height (m)	Wave period (s)	Tide (m)
2 March, 17:00	2.93	8.5	0.226
2 March, 17:20	3.55	9.1	0.226
2 March, 17:40	3.87	9.4	0.226
3 March, 8:00	3.09	9.4	0.076
3 March, 8:40	3.11	9.7	0.046
3 March, 9:00	2.91	9.7	0.026

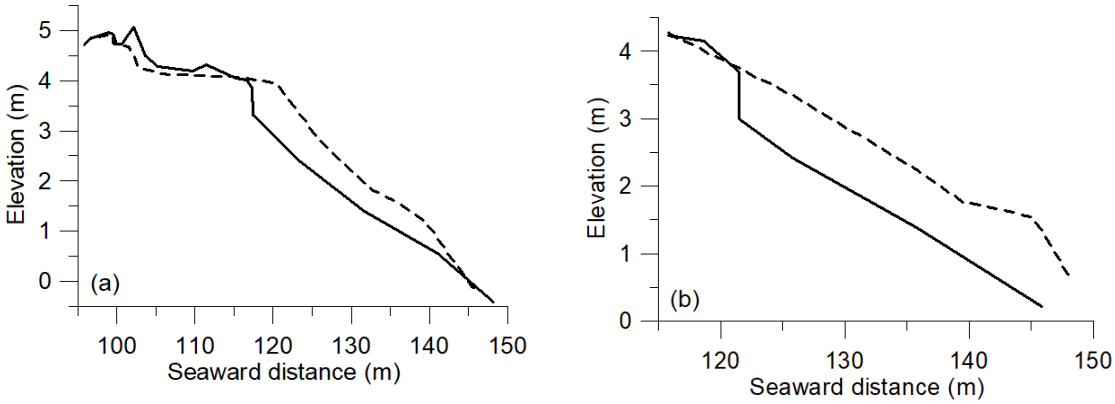

Figure 6 Berach profile changes from October (broken lines) to December (solid lines) in 2014 along (a) Line A and (b) Line B.

From October to December in 2014, a beach scarp was formed at the study site along Lines A and B (see the locations in Figure 1) as shown in Figure 6. We attributed this scarp formation to a severe storm that occurred from December 16 to 19. The maximum significant wave height and period measured seaward of the submerged breakwater at a water depth of approximately 12.0 m (see the location in Figure 1) was 6.73 m and 11.8 s, respectively, at 18:00 on December 17 (Figure 7 (a)). At that time, the sum of the tide measured in the West District of the Port of Niigata and the amount of wave setup measured shoreward of the submerged breakwater in Section B (see the location in Figure 1) was 0.81 m (Figure 7 (b)). Since the raw tidal data from the West District of the Port of Niigata showed a long period oscillation with an amplitude of approximately 0.4 m (figure not shown), the water level near the shoreline at the time of the maximum significant wave height was assumed to be 1.2 m.

We assumed that the beach scarp was formed by runup waves reaching the midpoint between the top and the bottom of the scarp, which was located at an average elevation of z = 3.5 m in Lines A and B. Considering the water level of 1.2 m near the shoreline at the time of the maximum significant wave height, the wave runup height measured in the field was assumed to be 2.3 m.

The comparison between the wave runup heights measured and estimated using the modified hypothetical slope method shows that the measured values were 25.5% larger than the estimated values on average (Figure 8). Thus, in the following procedures, the wave runup heights estimated using the modified hypothetical slope method will be multiplied by a factor of 1.25.

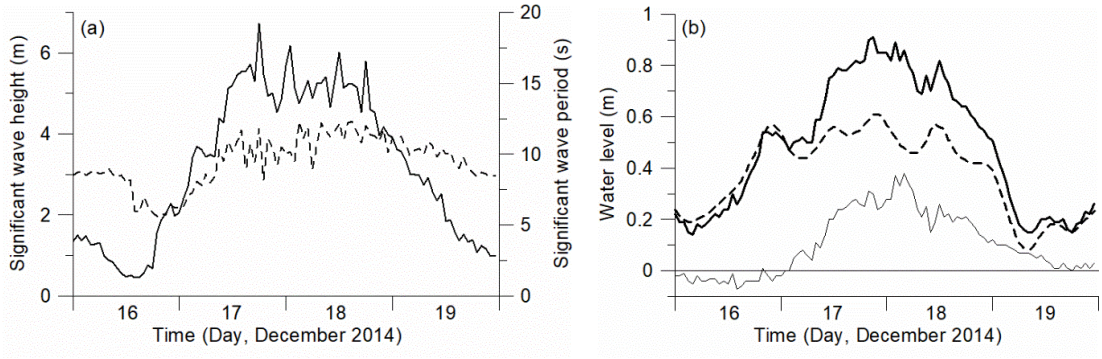

Figure 7 (a) Significant wave height (solid line) and period (broken line) measured shoreward of the submerged breakwater and (b) the tide measured in the West District of the Port of Niigata (broken line), the amount of wave setup measured in Section B (thin solid line) and the sum of the tide and the amount of wave setup (thick solid line).

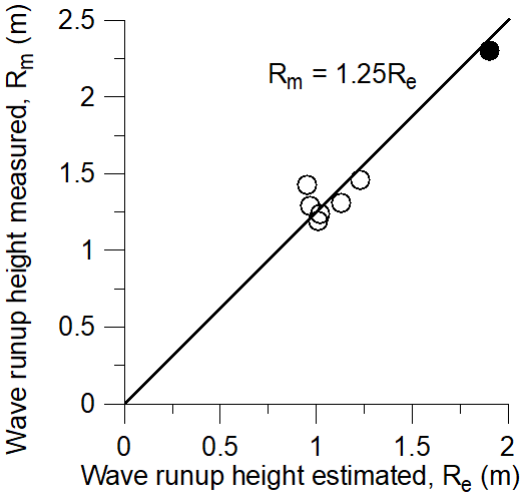

Figure 8 Comparison between the wave runup heights measured and estimated using the modified hypothetical slope method. The solid and open circles show the values in 2014 and 2021, respectively. The solid line represents the relationship of $R_m = 1.25R_e$.

Depth of closure

The depth of closure h_c, which was used in assuming eroded beach profiles, was estimated from the formula for critical water depth for completely active movement proposed by Sato (1966) based on distributions of radioactive tracers placed at the Kashima-nada Coast by Sato et al. (1963).

$$\frac{H_0}{L_0} = 2.4\left(\frac{d_m}{L_0}\right)^{1/3}\left(\frac{H_0}{H_c}\right)sinh\frac{2\pi h_c}{L_c} \qquad (5)$$

where H_0 is the offshore significant wave height, d_m is the sediment diameter, and H_c and L_c are the significant wave height and wavelength at the depth of closure. The significant wave height and period for waves with an occurrence probability of five times per year was used in the calculation; they were 4.5 m and 9.5 s, respectively. Over the submerged breakwater, the wave height was reduced to 2.7 m as the equivalent offshore significant wave height. The sediment diameter was set at 0.17 mm based on the measurement conducted just shoreward of the submerged breakwater in 2014. The obtained depth of closure was 9.04 m. Considering the amount of wave setup over the submerged breakwater induced by waves occurring five times per year, which was estimated to be 0.25 m, the elevation at the depth of closure at high water level (0.50 m) was calculated to be −8.29 m.

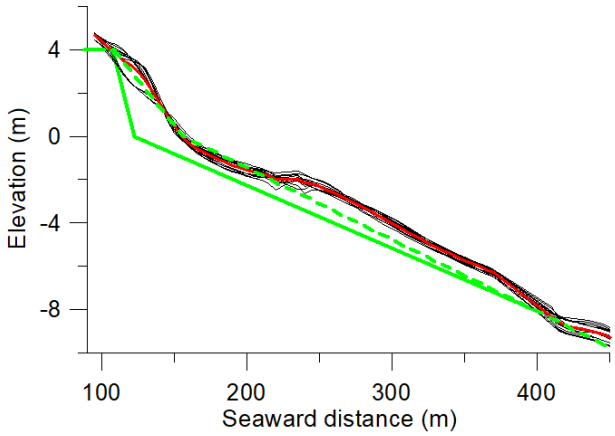

Figure 9 Mean beach profile (red line) and measured profiles (black lines) during a period from 2012 to 2020, assumed mean beach profile represented by four straight lines (green broken line) and beach profile with the critical beach width (green solid line).

Estimation of wave runup heights on assumed eroded beach profiles

Eroded beach profiles for determining the critical beach width were assumed using the mean beach profile from 2012 to 2020 (Figure 9), when the shoreline stabilized as shown in Figure 10. First, the mean beach profile was approximated by four straight lines as illustrated in Figure 9. One of the lines represents a flat backshore at z = 4.0 m, extending from y = 88 m (the seaward edge of the road, y is the seaward distance) to y = 108 m (Point A). The profile from Point A to the point at z = −8.0 m (Point B), located approximately at the depth of closure, was represented by two straight lines. One line connects Point A to the shoreline at z = 0 m (y = 156 m), while the other line connects the shoreline to Point B. Seaward of Point B, a straight line with a slope of 1/30 was assumed since the slope of the mean beach profile in the region from z = 0.0 m to −10.0 m was 1/31.5. Second, by assuming Points A and B to be fixed and varying the shoreline position at 10-m intervals, eroded beach profiles were created.

To estimate the wave runup heights at the shoreward edge of the backshore, the profiles from the shoreward edge of the backshore to the wave breaking points were used. When the wave runup height estimated on a profile with a vertical foreshore, in which the profile from the shoreline to the seaward edge of the backshore was vertical, was still lower than the road level, the critical beach width was set at the backshore width.

It was assumed that when the shoreline moves in accordance with sea level rise and land subsidence, the mean beach profile approximated by the straight lines would also shift in a corresponding manner. The profile would be maintained in relation to the low water level except for a decrease in the road level relative to the low water level. As the road level decreases, the wave runup height is more likely to exceed the road level, resulting in an increase in the critical beach width.

Prediction of future shoreline change

The future shoreline change was predicted using Eqs. (6) and (7), which are based on a simulation model developed by Kuriyama et al. (2012) and Kuriyama and Banno (2016).

$$y_{s,i} = y_{s,0} + \sum_{j=1}^{i} \left(\frac{dy_s}{dt}\right)_j \Delta t \qquad (6)$$

$$\left(\frac{dy_s}{dt}\right)_j = a_0 + a_1 + a_2 E_j^2 + a_3 E_j + a_4 (y_{s,j-1} - y_{eq,j-1}) \qquad (7)$$

where y_s is the shoreline position at z = 0.5 m, t is the time, a_0 is the geometrically obtained shoreline change rate due to sea level rise and land subsidence, which is (sum of the amounts of sea level rise and land subsidence)/(foreshore slope), a_1 to a_4 are coefficients to be calibrated, E is the offshore wave energy flux and y_{eq} is the amount of the shift of equilibrium profile from its initial position. The subscript j indicates the number of time steps.

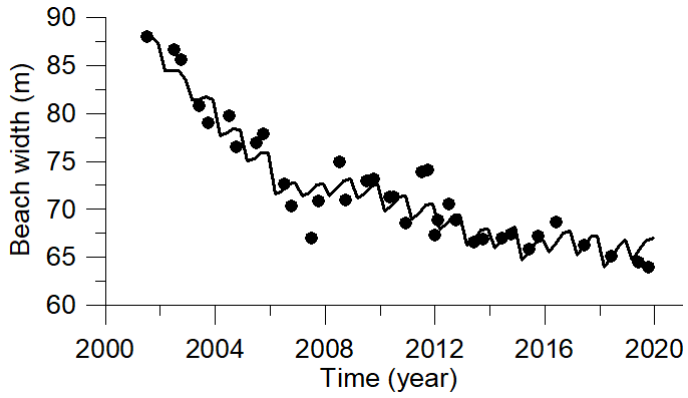

Figure 10 Beach widths measured (solid circles) and hindcasted (solid line) from 2001 to 2019.

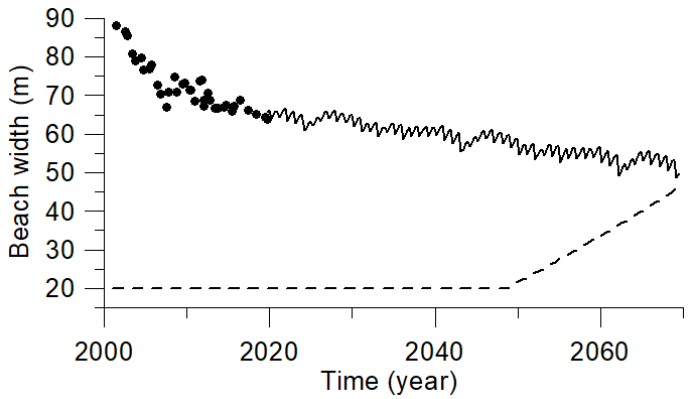

Figure 11 Beach widths measured in 2001 to 2019 (solid circles) and forecasted for 50 years from 2019 (solid line). The broken line shows the critical beach width.

The shoreline change rate, as expressed by Eq. (7), was assumed to be a function of the offshore wave energy flux and the shoreline position itself. The value of E was estimated with consideration of wave energy dissipation over the submerged breakwater as in Kuriyama and Banno (2016). The equilibrium profile was assumed to shift in parallel with sea level rise and land subsidence, and hence, the value of y_{eq} was assumed to be the sum of a_0.

In the calibration process, the data from July 2001 to October 2019 were used. Based on the morphological data, the foreshore slope was assumed to be 1/15 from July 2001 to June 2012 and 1/10 from July 2014 to October 2019. The slope between two periods was estimated by linear interpolation. The rate of land subsidence was assumed to be 7.0 mm/year based on field data, while the rate of sea level rise was set at 0. The time interval was 3 months as in Kuriyama and Banno (2016). The coefficients of a_1 to a_4 were determined using the SCE-UA method (Duan et al., 1983) so that the error between the measured and estimated shoreline positions was minimal.

The future shoreline change for a period of 50 years starting in June 2019 was predicted using the calibrated coefficients. The rate of sea level rise was set at 4.11 mm/year (= 0.39 m/95 years), which is the value for the RCP2.6 scenario in SROCC (Oppenheimer et at., 2019). The amount of subsidence was set at 7.0 mm/year as in the calibration. The foreshore slope was assumed to be 1/12.5 based on the recent morphological data. The offshore wave heights and periods measured from 2001 to 2019 repeated 2.6 times during the forecast period.

RESULTS AND DISCUSSION

The design significant wave height was reduced from 9.3 m at a water depth of 35 m to 5.9 m at the seaward edge of the submerged breakwater and to 3.5 m at its shoreward edge. The depth of wave breaking was calculated to be 7.9 m based on Goda's formula on wave breaking (Goda, 1985).

The estimated critical beach width, which is the distance from the seaward edge of the road to the shoreline at high water level, was 20.0 m in 2019. It is expected to begin increasing in 2049 and to reach 46.3 m in 2069 (Figure 9).

The coefficient values obtained in the calibration process were $a_1 = 1.6086 \times 10^{-6}$ (m/day), $a_2 = -9.2242 \times 10^{-10}$ ((m s^2)/(N^2 day)), $a_3 = -3.2203 \times 10^{-11}$ ((m s)/(N day)) and $a_4 = -5.9826 \times 10^{-4}$ (1/day). The shoreline positions from 2001 to 2019 estimated using the obtained coefficients agreed well with the measured ones (Figure 10). The root-mean-square error was 1.94 m.

Over the 50-year period starting in June 2019, the shoreline is expected to retreat 14.9 m (Figure 11). However, this retreat will not reach the critical value, confirming the effectiveness of the disaster prevention function of the nourished beach at the study site for the next 50 years even under conditions of sea level rise and land subsidence.

In this study, the future change of waves due to global warming was not considered as in Kuriyama and Banno (2016) because Hemer et al. (2013) and Shimura (2015) showed that waves will not significantly change off the study site for the next 100 years. Although tropical cyclones (typhoons) are predicted to become more intense due to global warming, their impact on the future wave climate off the study site is likely to be limited as the study site is currently infrequently affected by typhoons. However, if an intensified typhoon strikes the study site, it would cause significant damage to the beach. Therefore, regular and timely monitoring of the beach including measurements of shoreline position and observations of beach scarp formation is strongly recommended.

CONCLUSIONS

In this study, we investigated whether a nourished beach on the Niigata West Coast in Japan can maintain its disaster prevention function over a 50-year period under conditions of sea level rise and land subsidence. First, we defined the disaster prevention function of the nourished beach as the ability to prevent the wave runup height from exceeding the level of the road behind the beach. Second, the critical beach width, which was defined as the minimum width to satisfy the criterion of the disaster prevention function, was determined by assuming eroded beach profiles based on morphological data and by estimating the wave runup heights for these profiles using the modified hypothetical slope method.

Third, we predicted future shoreline change for the next 50 years using a numerical simulation model, which was calibrated and evaluated using the data obtained during a period from 2001 to 2019. In the future shoreline prediction, the rate of land subsidence was assumed to be 7.0 mm/year and the rate of sea level rise was set at 4.1 mm/years, which is the value for the RCP2.6 scenario in SROCC. The shoreline is expected to retreat by 14.7 m over the 50 years but will not reach the critical value. This prediction confirmed that the disaster prevention function of the nourished beach will remain effective for the next 50 years even under conditions of sea level rise and land subsidence.

Although the future wave changes due to global warming were not considered in this study based on previous studies on wave climate change, an intensified typhoon, which was projected to occur, could significantly damage the beach in the future. Therefore, it is crucial to conduct regular monitoring of the beach including shoreline position measurement and beach scarp observation.

ACKNOWLEDGMENTS

The measured offshore wave data were provided by the Ports and Harbours Bureau, Ministry of Land, Infrastructure, Transport and Tourism, and Port and Airport Research Institute. The tidal data were offered by Japan Oceanographic Data Center (https://www.jodc.go.jp/jodcweb/JDOSS/index.html).

REFERENCES

Duan, Q.Y., V.K. Gupta, and S. Sorooshian. 1993. Shuffled complex evolution approach for effective and efficient global minimization, *Journal of Optimization Theory and Applications*, 73(3), 501-521.

Goda, Y. 1985. *Random seas and design of maritime structures*, University of Tokyo Press, Tokyo, Japan, 323p.

Hemer, M.A., Y. Fan, N. Mori, A. Semedo, and X.L. Wang. 2013. Projected changes in wave climate from a multi-model ensemble, *Nature Climate Change*, 3, 471‑476.

Kishi, H., M. Tamuro, K. Mizuuchi, K. Yamakawa, and Y. Oyamatsu. 2013. Hydrological characteristics on the double row submerged-breakwater under consideration in Niigata West Coast, *Journal of*

Japan Society of Civil Engineers B2 (Coastal Engineering), 60(2), I_1001-I_1005. (in Japanese with English abstract)

Kuriyama, Y., S. Yamaguchi, M. Ikegami, S. Takano, and J. Tanaka. 2006. Morphological changes around large-scale submerged breakwater on the Niigata coast, Japan, *Proceedings of 30th International Conference on Coastal Engineering*, ASCE, 3695-3707.

Kuriyama, Y., M. Banno, and T. Suzuki. 2012. Linkages among interannual variations of shoreline, wave and climate at Hasaki, Japan, *Geophysical Research Letters*, 39, L06604.

Kuriyama, Y., and M. Banno. 2016. Shoreline change caused by the increase in wave transmission over a submerged breakwater due to sea level rise and land subsidence, *Coastal Engineering*, 112, 9-16.

Nakamura, M., Y. Sasaki, and J. Yamada. 1972. Wave runup of composed cross section, *Proceedings of 11th Japanese Conference on Coastal Engineering*, JSCE, 309-312. (in Japanese)

Okuda, S., T. Watanabe, T. Tanaka, T. Hiraike, and A. Katano. 2017. Soundness indicators for sandy beach maintenance, *Journal of Japan Society of Civil Engineers B2 (Coastal Engineering)*, 73(2), I_1567-I_1572. (in Japanese with English abstract)

Oppenheimer M., and others. 2019. Sea Level Rise and Implications for Low-Lying Islands, Coasts and Communities, *IPCC Special Report on the Ocean and Cryosphere in a Changing Climate*, edited by H.-O. Pörtner and others, Cambridge University Press, Cambridge, UK and New York, NY, USA, 321-445.

Sato, S. 1966. Littoral drift, *Lecture Notes of the Summer Seminar on Hydraulic Engineering, 1966, Course B*, JSCE, 19.1-19.29. (in Japanese)

Sato, S., T. Ijima, and N. Tanaka. 1963. A study of critical depth and mode of sand movement using radioactive glass sand, *Proceedings of 8th International Conference on Coastal Engineering*, ASCE, 304-323.

Seacoast Office of River Bureau of Ministry of Land, Infrastructure, Transport and Tourism, and Coast Division of National Institute of Land and Infrastructure Management. 2004. *Design manual for artificial reefs (revised edition)*, National Association of Sea Coast, 95p. (in Japanese)

Shimura, T. 2015. *Long term projection of ocean wave climate and its climatic factors*, Dissertation Kyoto University, Kyoto University, Japan, 106p.